The automation of the image possessing and calculation of indices by means of EASI Modelling in Python (PCI Geomatics)

Report to performed internship

at the Centre for Geographical Analysis (CGA, Stellenbosch University)

from 02.09.2017 until 08.02.2018

From: Linara Arslanova (165910)

To: Dr. Christian Berger

Date: 27.02.2018

Table of contents

I List of Figures

II List of Tables

III Introduction

During the internship at the Centre for Geographical Analysis[1] (CGA) in the period from September 2017 to February 2018 the moderate resolution Landsat-8 data was used to retrieve vegetation indices. As a result, these created products will be used further in the biomass mapping. This Internship was conducted as a part of the ARS AfricaE project (FKZ: 01LL1303). In collaboration with four German and six South African partner institutions, ARS AfricaE investigates the coupled carbon and water cycles of natural and disturbed savanna ecosystems in Southern Africa (ARS AFRICA E, 2014).

The main focus of the work was on automation of the image processing by means of PCI Geomatics and Python. Follow tasks was working out:

- data collection
- literature review for choosing appropriate cloud masking and mosaic creation techniques
- cloud/water masking
- creation of mosaic compositions for one path
- calculation of vegetation indices and creation of mosaic compositions for the entire investigation area (Kruger National Park);

The IDLE Python IDE (Python 2.7.14) was used to create the batch-scripts, as well as Geomatica *Python* API (2017).

In this report the methods considered for image pre-processing (cloud and water body masking) will be described and the chosen methods justified.

The report discusses the following topics:

- data collection (Landsat 8 Level-2)
- cloud and water masking
- mosaicking
- calculation of indices
- batch processing

To choose appropriate pre-processing steps for Landsat 8 Level 2 images Lück und van Niekerk (2016), Ganie und Nusrath (2016), and Young et al. (2017) were studied. However, mainly the paper from Young et al. (2017) was used. In his paper an overview to Landsat 8 products and to potential prepossessing methods was given. Commonly used terminology

[1] Stellenbosch University, cooperation partner under ARS AfricaE Project

was clarified and a decision tree to define the correct pre-processing workflow was presented.

Investigation area

The investigation area is located in north-eastern part South Africa's (Fig.1) which has two distinct seasons: the rainy season (from November to March) and the dry season (from May to September). The rainfalls are mostly associated with tropical-temperate troughs and easterly tropical airs flow over the interior, resulting in warm and humid summers (most rain in December - February) (Grab and Knight 2015). In contrast, the cold, dry conditions during winter (June to August) are a result of the high-pressure system that dominates over the interior (Grab and Knight 2015). The study area is located east of the Great Escarpments causes regional and microscale changes in precipitation, humidity, airflow and temperature (Grab and Knight 2015). The Region has mean annual precipitation variations of between 500 mm to 1200 mm (Grab and Knight 2015). The difference in height is 500 m with distinct gradient from east to west.

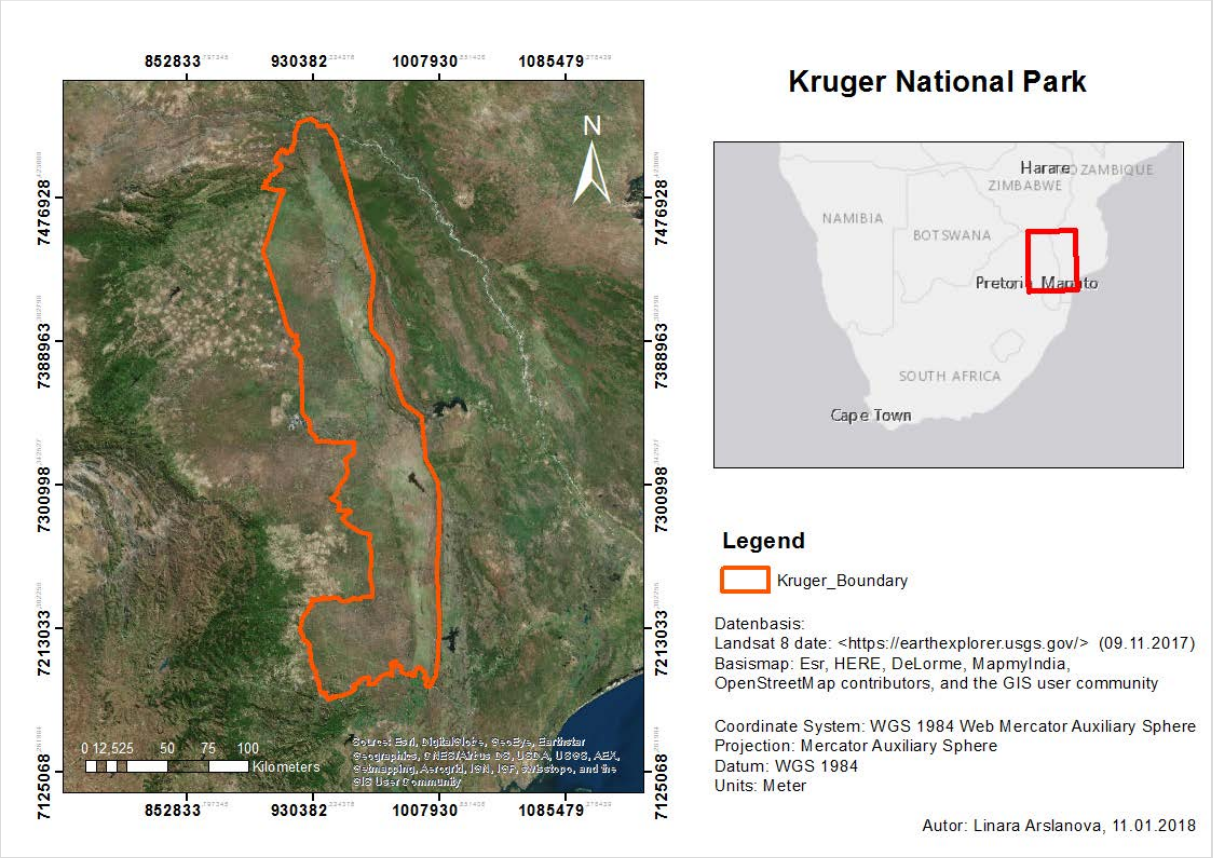

Fig.1: Study area.

1 Data collection (Landsat 8 Level-2)

A Surface Reflectance product (LaSR[2]) is a high quality data that has been preprocessed from the United States Geological Survey (USGS) to a level of relative correction. LaSR data was processed to calibrate raw Digital Numbers (DN) to top-of-atmosphere (TOA) reflectance, and then corrected to a surface reflectance using atmospheric parameters and a Digitally Elevated Model (DEM). Thus, the higher-Level 2 data is orthorectified, radiometrically and atmospheric corrected imagery (USGS, 20017), defined in the Universal Transverse Mercator (UTM) map projection and equivalent to the World Geodetic System (WGS84) (Young et al. 2017).

This data was selected, ordered and downloaded through the United States Geological Survey (USGS), EarthExplorer website <earthexplorer.usgs.gov> (EARTH EXPLORER, 2017). The Landsat 8 images are acquired for 16-days repeat cycles and have an approximate scene size of 185 km in north-south and 180 km in east-west. The LaSR product contains all bands except Panchromatic Band 8, Cirrus Band 9, and Thermal Bands 10 and 11, delivered in a 16-bit unsigned integer format and having a spatial resolution of 30m. Each LaSR band are stored in a separate condition specific file (*sr_band1.tif, sr_band2.tif…*) available with metadata file (*.xml*) and a Level-2 Pixel Quality Assurance (PQA) band (*_pixel_qa.tif*) which contains the information about clouds, water or snow, which can be used for masking (USGS, 2017). The product also contain another ancillary files that had not been used in this work (for more information about ancillary data see Jenkerson (2017)).

The USGS LaSR data is highly recommended for calculation of vegetation indices (Young et al. 2017). Because this data have high level of image processing and it eliminate the need for the user to complete pre-processing steps, that can introduce additional errors (Jenkerson 2017 ; Young et al. 2017). On the other hand, the process to develop LaSR products contains nonlinear elements, which can introduce error and unwanted data artifacts (Young et al. 2017), especially it is relevant for coastal regions (Jenkerson 2017).

Nine months-periods from September 2016 to October 2016 were selected for serial time analysis (Tab.3). Five images were required (path 168-169 and row 76-78) to cover the entire investigation area (Fig.2). The obtaining of cloud free imagery for the index calculation was challenging, images with less than 10% cloud cover preferably were chosen. However images with greater cloud cover could be suitable for uses as well. For instance, when the cloud concentration is located outside the investigation area (example shown on Fig.2). Therefore images below 20% cloud cover were chosen for the index calculation (Tab.3).

[2] Example of the name downloaded Landsat-8 imagery (Band 1) : LC08_L1TP_168076_20161006_20170320_01_T1_sr_band1.tif

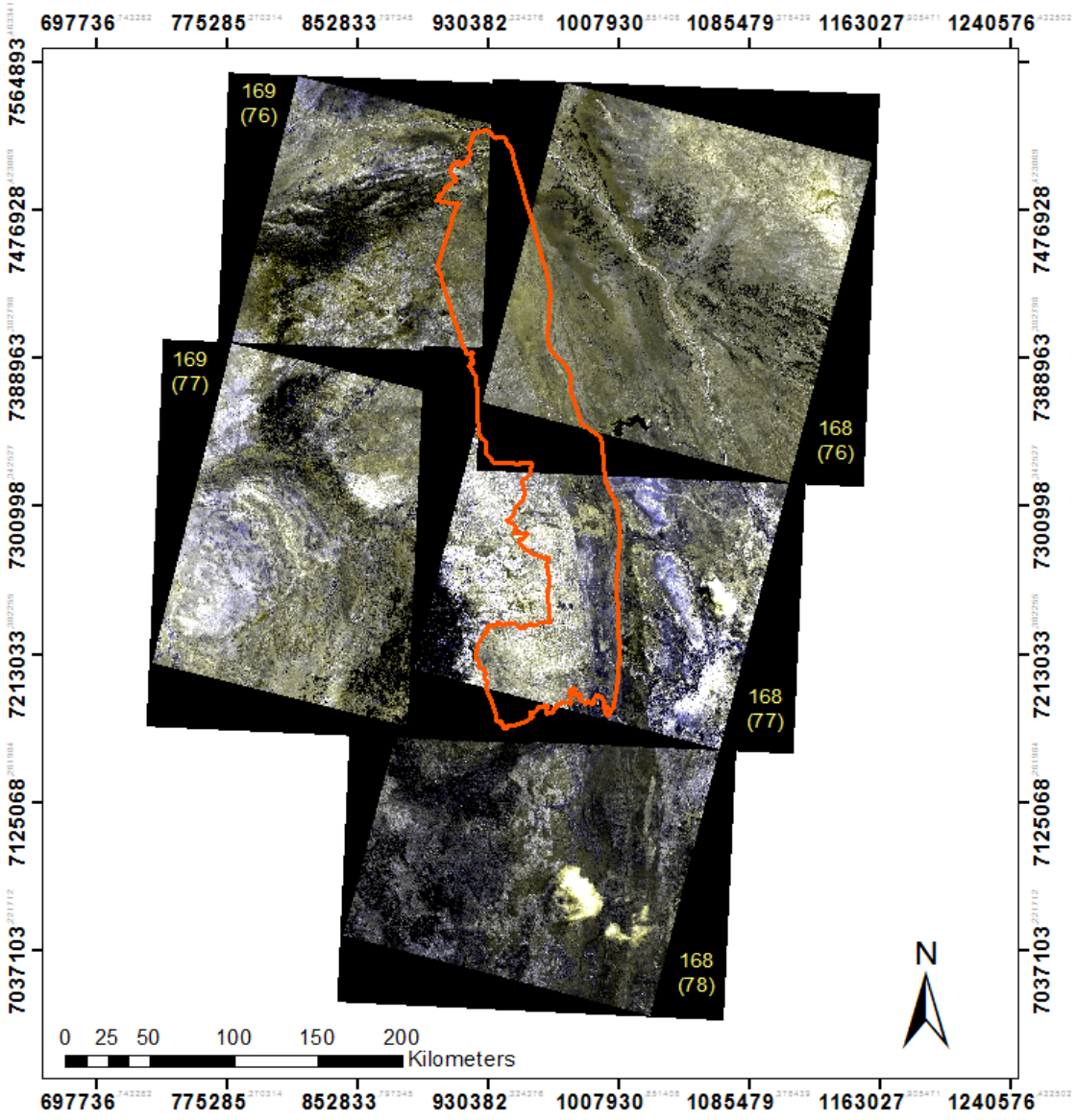

Legend

Kruger_Boundary

LC08_L1TP_168076_20161006_20170320_01_T1_sr_MS_orig.pix

RGB

Red: Band_1

Green: Band_2

Blue: Band_3

Datenbasis:
Landsat 8 date: <https://earthexplorer.usgs.gov/> (09.11.2017)
Basismap: Esr, HERE, DeLorme, MapmyIndia, OpenStreetMap contributors, and the GIS user community

Coordinate System: WGS 1984 UTM Zone 35S
Projection: Transverse Mercator
Datum: WGS 1984
Units: Meter

Autor: Linara Arslanova, 11.02.2018

Fig.2: An example of the selected Landsat 8 data product band files.
Location of paths and rows. Composites (Violet/Blue, Blue, Green).

2. Cloud and water masking

Before calculation of vegetation indices, cloud and water body masking should be performed, because the calculation over pixels containing clouds will show anomalous values (PCI GEOMATICA, 2017; Young et al. 2017; USGS, 20017).

Listed below are methods that were considered for generating cloud mask for Landsat 8 imagery:

- *The Level-2 Quality Assurance band.* As mentioned before, this band contains quality information about cloud, snow/ice, and water bodies that is derived with using a CFMask[3] algorithm. It is highly recommended to use masks delivered with Landsat 8 Level-2 product (Foga et al. 2017; Young et al. 2017). Because CFMask algorithm shows the best overall accuracy among the many algorithms that was considered by USGS to implement for Landsat products (Foga et al. 2017). Each pixel in this band is represented as an integer that contains bit-packed combinations of surface, atmosphere, and sensor conditions (USGS, 20017).
    - These combinations could be "unpacked" by using the *Landsat-8 Quality Assessment Tools*, which has been developed by USGS and is provided without charge for download on webpage <https://landsat.usgs.gov/landsat-qa-tools> (USGS, 20017).
    - Another way to extract the mask from PQA band is to use *Geomatica's Platform Python API and NumPy package*. Geomatica's Platform Python API allows access the PQA raster as a NumPy array and to perform new value coding. The water body/cloud mask was generated using this method. The value 1 was coded for cloud and water values and value 0 for the rest of information.

- *Generating of masks by using algorithm presented in PCI Geomatica.* Cloud, haze, water body masks can be generated automatically by using *masking()* function. Function *hazerm()* allows to remove haze from image on the basis generated masks in a previous step. Although under this method water bodies have not been detected properly. As input parameter for *masking()* and *hazerm()* function the CLOUD_TRESH = [14, 22, 1], HAZECOV = [30] and WUTHRESH = [5,3] was set up, which corresponds to haze cover 50%. These thresholds were chosen by experimenting on the values to produce the best cloud mask.

[3] CFMask, was originally developed at Boston University in a Matrix Laboratory (MATLAB) environment to automate cloud, cloud shadow, and snow masking for Landsat TM and ETM+ images (Jenkerson 2017).

3. Mosaicking

Mosaicking of images from different acquisition dates before the index calculation will reduce accuracy of results (Young et al. 2017). This happens because mosaicking includes *relative radiometric correction (normalisation) that* brings each band of the image to the same radiometric scale as the corresponding band of a reference image. If the plants are at different development stages during image aquisition, application of the relative radiometric correction during their mosaicking will lead to the initial (true) values of the images being averaged. Especially it is typical for the investigation area with clearly distinct season's transition, where intensive rainfall after dry seasons will cause intensive vegetation growth and flowering. Therefore, images acquired from the same day (one path) were mosaicked before the index calculation and after mosaic compositions from two paths were mosaicked without normalisation (Fig.4).

To create seamless mosaic and even out colour contrasts between images the '*Bundle*' method with an '*Adaptive*'-filter (function from PCI Geomatica) was used. The filter adjusts the brightness and contrast over local areas by reducing the bright-and-dark pattern over the entire image and leading to improved image details (PCI GEOMATICA, 2017). Image mosaicking was performed by using function presented in PCI Geomatica: *mosprep(), mosdef(), mosrun().*

The '*Bundle*' colour balancing method is performed in two steps. Initially, statistics will be calculated for all overlapping image areas, after which colour balancing will be applied. Clouds, snow etc. will be excluded before colour adjustment (PCI GEOMATICA, 2017).

Another colour balancing approach is '*histogram matching*'. Initially the histogram is built for each image starting from the centre of the mosaic. The optimum radiometry of the input image is then determined and applied to the entire input image as it is added to the mosaic (PCI GEOMATICA, 2017).

Both approaches ('*bundle*' and '*histogram matching*') are recommended to use for relative correction of multiple images acquired on the same day (one path), where variations in solar and atmospheric conditions are insignificant. (Roy et al. 2014).

To achieve good results in *colour balancing* during automatic image mosaicking with PCI Geomatica, an implementation of a water body mask is also important for the setting cut lines (PCI GEOMATICA, 2017).

4 Calculation of Indices

Before vegetation indices were calculated, cloud and water body masks were burned into the atmospheric corrected image using PCI Geomatica function *burnmask().* The 72 indices were calculated (Tab.1), collected from the following website <www.indexdatabase.de> (INDEX DATA BASE, 2017). On the website all vegetation indices are listed that possible to calculate from Landsat 8 data. Three methods to calculate vegetation indices with PCI Geomatica were considered:

- using function *vegindex()*
- using function *ari()*
- or using *Geomatica's Platform Python API* and *NumPy*

Function *ari()* allows arithmetical operation between two channels only and masks pixel to process. Function *vegindex()* allows the calculation of only 12 vegetation indices from the required. Geomatica's Platform Python API allows access to the raster as a NumPy array and to perform the calculation with multiple channels (NumPy arrays). This method was implemented to the index calculation. The "no_value" and cloud/water pixels were set to value -9999.

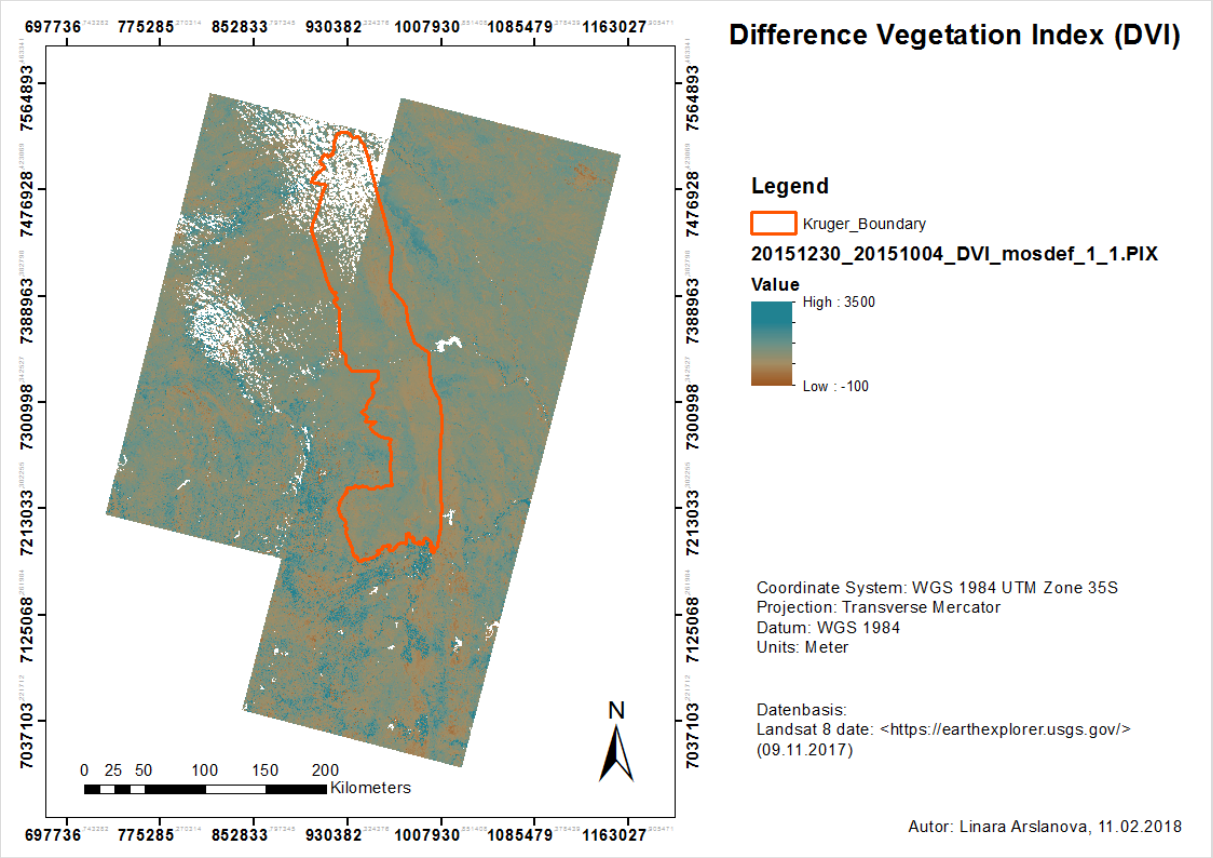

Fig.3: An example of the calculated vegetation index.

5. Batch processing

The LaSR Products are delivered in a tar.gz compressed files. To unzipp gzip files (.tar.gz) the script *unzip.py* was written.
The following structure of python scripts for indices calculation is presented:

1. *main.py*
2. *util.py*
3. *indices.py*

The script *indice.py* content functions and formulas of vegetation indices that could be extended in the amount.

The *main.py* script contains workflow to the image processing:

1. setting the working directory
2. creating working folders with names according to unique names of images.
3. workflow to the Image processing.
   - import files from *.tif* format to *.pix* format
   - channel stacking
   - extracting cloud and water masks from PQA
   - burning masks into images
4. mosaic preparation and image mosaicking of the same paths for further calculation of indices
5. calculation of indices
6. mosaic of two paths to one composition, output in *.tif* format

The script *utils.py* contains the function that is required for executing the main script.

The final mosaic composition has *.tif* format, 30 m spatial resolution and 32-bit (floating point values) radiometric resolution.

6. Outlook

There is a need for validation of created products. This can be performed through comparisons with USGS products and in-situ available data, as well as retrieving of Land Surface Temperature (LST), calculations of Principal Component Analysis (PCA), Tassel Cap brightness (TC) and performing of Texture Analysis(TA). These calculations require images acquired from the Thermal Infrared Sensor (TIRS).

III List of references

Foga, Steve; Scaramuzza, Pat L.; Guo, Song; Zhu, Zhe; Dilley, Ronald D.; Beckmann, Tim et al. (2017): Cloud detection algorithm comparison and validation for operational Landsat data products. In: *Remote Sensing of Environment* 194, S. 379–390. DOI: 10.1016/j.rse.2017.03.026.

Ganie, MushtaqAhmad; Nusrath, Dr.Asima (2016): Determining the Vegetation Indices (NDVI) from Landsat 8 Satellite Data. In: *IJAR* 4 (8), S. 1459–1463. DOI: 10.21474/IJAR01/1348.

Grab, Stefan; Knight, Jasper (Hg.) (2015): Landscapes and landforms of South Africa. Cham, Heidelberg, New York, Dordrecht, London: Springer (World geomorphological landscapes).

Jenkerson, Calli (2017): PRODUCT GUIDE LANDSAT 8 SURFACE REFLECTANCE CODE (LASRC) PRODUCT. In: *Department of the Interior* Version 4.2. Online verfügbar unter https://landsat.usgs.gov/sites/default/files/documents/lasrc_product_guide.pdf.

Lück, W.; van Niekerk, A. (2016): Evaluation of a rule-based compositing technique for Landsat-5 TM and Landsat-7 ETM+ images. In: *International Journal of Applied Earth Observation and Geoinformation* 47, S. 1–14. DOI: 10.1016/j.jag.2015.11.019.

Roy, D. P.; Wulder, M. A.; Loveland, T. R.; C.E., Woodcock; Allen, R. G.; Anderson, M. C. et al. (2014): Landsat-8. Science and product vision for terrestrial global change research. In: *Remote Sensing of Environment* 145, S. 154–172. DOI: 10.1016/j.rse.2014.02.001.

Young, Nicholas E.; Anderson, Ryan S.; Chignell, Stephen M.; Vorster, Anthony G.; Lawrence, Rick; Evangelista, Paul H. (2017): A survival guide to Landsat preprocessing. In: *Ecology* 98 (4), S. 920–932. DOI: 10.1002/ecy.1730.

Ganie, M; Nusrath, A. (2016): Determining the Vegetation Indices (NDVI) from Landsat 8 Satellite Data. In: *IJAR* 4 (8), S. 1459–1463. DOI: 10.21474/IJAR01/1348.

Grab, S.; Knight, J. (Hg.) (2015): Landscapes and landforms of South Africa. Cham, Heidelberg, New York, Dordrecht, London: Springer (World geomorphological landscapes).

Lück, W.; van Niekerk, A. (2016): Evaluation of a rule-based compositing technique for Landsat-5 TM and Landsat-7 ETM+ images. In: *International Journal of Applied Earth Observation and Geoinformation* 47, S. 1–14. DOI: 10.1016/j.jag.2015.11.019.

Roy, D. P.; Wulder, M. A.; Loveland, T. R.; C.E., Woodcock; Allen, R. G.; Anderson, M. C. et al. (2014): Landsat-8. Science and product vision for terrestrial global change research. In: *Remote Sensing of Environment* 145, S. 154–172. DOI: 10.1016/j.rse.2014.02.001.

Young, N. E.; Anderson, R. S.; Chignell, S. M.; Vorster, A. G.; Lawrence, R.; Evangelista, P. H. (2017): A survival guide to Landsat preprocessing. In: *Ecology* 98 (4), S. 920–932. DOI: 10.1002/ecy.1730.

Internet sources:

ARS AFRICA E (2014): Adaptive Resilience of Southern African Ecosystems <https://ars-africae.org/> (last accessed on 25.08.2017)

EARRH EXPLORER (2017): EarrhExplorer – USGS. < https://earthexplorer.usgs.gov/ > (last accessed on 15.11.2017).

FMASK (2011): fmask software. <https://code.google.com/archive/p/fmask/> (last accessed on 12.12.2017)

HaoliangYu.io (2015): Generating masks from Landsat 8 image in ArcMap. <http://haoliangyu.github.io/2015/05/08/Generating-masks-from-Landsat-8-image-in-ArcMap/

https://landsat.usgs.gov/landsat-qa-tools> (last accessed on 5.11.2017)

PCI GEOMATICA (2017): PCI Geomatics. < www.pcigeomatics.com> (last accessed on 6.02.2018)

INDEX DATA BASE (2017): Index DataBase. A database for remote sensing indices. <https://www.indexdatabase.de/> (last accessed on 6.02.2018)

USGS (20017): USGS Landsat Mission. <https://landsat.usgs.gov/> (last accessed on 30.10.2017)

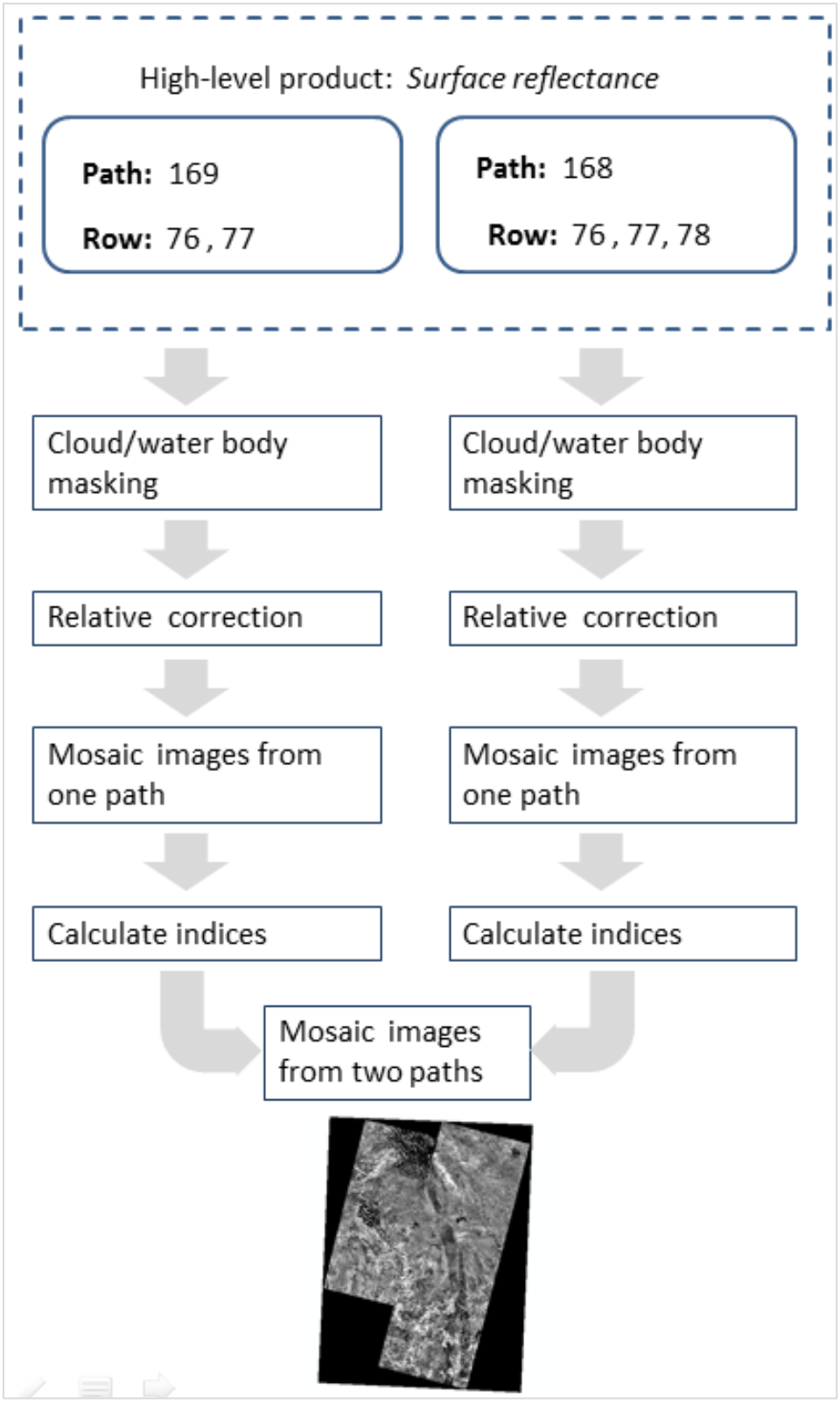

used PCI Geomatics functions

fimport()

pcimod()

iii()

burnmask()

mosprep()

mosedef()

mosran()

packages numpy, pci.api.gobs/datasource

mosprep()

mosedef()

mosran()

Fig.4: Automated image processing workflow

Tab.1: Collection of vegetation Indices from different webpages

N	Index	Description	Source
1	AFVI600	Aerosol Free Vegetation Index 1600	https://www.indexdatabase.de/db/s-single.php?id=168
2	ARVI	Atmospheric Resistant Vegetation Index	http://grass.osgeo.org/grass70/manuals/i.vi.html
3	ARVI2	Atmospherically Resistant Vegetation Index 2	https://www.indexdatabase.de/db/s-single.php?id=168
4	AVI	Ashburn Vegetation Index	https://www.indexdatabase.de/db/s-single.php?id=168
5	BWDRVI	Blue-Wide Dynamic Range Vegetation Index	https://www.indexdatabase.de/db/s-single.php?id=168
6	CHL1	Chlorophyll 1 Index	by Fabian Faßnacht, 2011
7	CHL2	Chlorophyll 2 Index	by Fabian Faßnacht, 2011
8	CHLIG	Chlorophyll Index Green	https://www.indexdatabase.de/db/s-single.php?id=168
9	CHLVI	Chlorophyll Vegetation Index	https://www.indexdatabase.de/db/s-single.php?id=168
10	CI	Coloration Index	https://www.indexdatabase.de/db/s-single.php?id=168
11	CRI1	Carotenoid Reflectance Index 1	by Fabian Faßnacht, 2011
12	CTVI	Corrected Transformed Vegetation Index	https://www.indexdatabase.de/db/s-single.php?id=168
13	DNG	Difference Nir/Green	https://www.indexdatabase.de/db/s-single.php?id=168
14	DVI	Difference Vegetation Index	http://grass.osgeo.org/grass70/manuals/i.vi.html
15	DVIMSS	Differenced Vegetation Index Mss	https://www.indexdatabase.de/db/s-single.php?id=168
16	EVI	Enhanced Vegetation Index For High Biomass Regions Only	http://grass.osgeo.org/grass70/manuals/i.vi.html
17	EVI2	Enhanced Vegetation Index 2	http://grass.osgeo.org/grass70/manuals/i.vi.html
18	GARI	Green Atmospherically Resistant Vegetation Index	http://grass.osgeo.org/grass70/manuals/i.vi.html
19	GBNDVI	Green-Blue Ndvi	https://www.indexdatabase.de/db/s-single.php?id=168
20	GEMI	Global Environmental Monitoring Index	http://grass.osgeo.org/grass70/manuals/i.vi.html
21	GLI	Green Leaf Index	https://www.indexdatabase.de/db/s-single.php?id=168

Tab.1-2

22	GNDVI	Green Normalized Difference Vegetation Index	https://www.indexdatabase.de/db/s-single.php?id=168
23	GOSAVI	Green Optimized Soil Adjusted Vegetation Index	https://www.indexdatabase.de/db/s-single.php?id=168
24	GRNDVI	Green-Red Ndvi	https://www.indexdatabase.de/db/s-single.php?id=168
25	GRVI1	Green-Red Vegetation Index 1	from SNAP Sentinel 5
26	GSAVI	Green Soil Adjusted Vegetation Index	https://www.indexdatabase.de/db/s-single.php?id=168
27	GVI	Green Vegetation Index	http://grass.osgeo.org/grass70/manuals/i.vi.html
28	GVMI	Global Vegetation Moisture Index	https://www.indexdatabase.de/db/s-single.php?id=168
29	HUE	Hue	https://www.indexdatabase.de/db/s-single.php?id=168
30	INTENSITY	Intensity	https://www.indexdatabase.de/db/s-single.php?id=168
31	IPVI	Infrared Percentage Vegetation Index. On The Website From Grass.Osgeo Another Formel	http://grass.osgeo.org/grass70/manuals/i.vi.html
32	LAI-SAVI	Leaf Area Index- Soil Adjusted Vegetation Index	from SNAP Sentinel 4
33	MIVI	Mid-Infrared Vegetation Index	https://www.indexdatabase.de/db/s-single.php?id=168
34	MSAVI	Modified Soil Adjusted Vegetation Index	http://grass.osgeo.org/grass70/manuals/i.vi.html
35	MSI	Moisture Stress Index.	from SNAP Sentinel 3
36	MSR	Modified Simple Ratio Nir/Red	https://www.indexdatabase.de/db/s-single.php?id=168
37	NDGRINBLUE	Normalized Difference 550/450	https://www.indexdatabase.de/db/s-single.php?id=168
38	NDGRINRED	Normalized Difference 550/650	https://www.indexdatabase.de/db/s-single.php?id=168
39	NDNIRBLUE	Normalized Difference Nir/Blue	https://www.indexdatabase.de/db/s-single.php?id=168
40	NDNIRGREEN	Normalized Difference Nir/Green	https://www.indexdatabase.de/db/s-single.php?id=168
41	NDNIRSWIR1	Normalized Difference 860/1640	https://www.indexdatabase.de/db/s-single.php?id=168

Tab.1-3

42	NDNIRSWIR2	Normalized Difference Nir/Mir	https://www.indexdatabase.de/db/s-single.php?id=168
43	NDREDGREEN	Normalized Difference Red/Green	https://www.indexdatabase.de/db/s-single.php?id=168
44	NDVI	Normalized Difference Vegetation Index.	http://grass.osgeo.org/grass70/manuals/i.vi.html
45	NDVIREDBLUE	Red-Blue Ndvi	https://www.indexdatabase.de/db/s-single.php?id=168
46	NDWI	Normalized Difference Water Index	https://www.indexdatabase.de/db/s-single.php?id=168
47	NG	Norm G	https://www.indexdatabase.de/db/s-single.php?id=168
48	NNIR	Norm NIR	https://www.indexdatabase.de/db/s-single.php?id=168
49	NR	Norm R	https://www.indexdatabase.de/db/s-single.php?id=168
50	OSAVI	Optimised Soil Adjusted Vegetation Index	https://www.indexdatabase.de/db/s-single.php?id=168
51	PANNDVI	Pan NDVI	https://www.indexdatabase.de/db/s-single.php?id=168
52	PSIR-NIR	Plant Senescence Reflectance Index-Near Infra-Red	from SNAP Sentinel 2
53	RDVI	Renormalized Difference Vegetation Index	by Fabian Faßnacht, 2011
54	SARVI2	Soil And Atmospherically Resistant Vegetation Index 2	https://www.indexdatabase.de/db/s-single.php?id=168
55	SHPINDEX	Shape Index	https://www.indexdatabase.de/db/s-single.php?id=168
56	SIPI	Structure Intensive Pigment Index.	from SNAP Sentinel 2
57	SLAVI	Specific Leaf Area Vegetation Index	https://www.indexdatabase.de/db/s-single.php?id=168
58	SRCOASTGREEN	Simple Ratio 450/550	https://www.indexdatabase.de/db/s-single.php?id=168
59	SRGRINRED	Simple Ratio 550/670	https://www.indexdatabase.de/db/s-single.php?id=168
60	SRNIRGREEN	Simple Ratio Nir/G	https://www.indexdatabase.de/db/s-single.php?id=168

Tab.1-4

61	SRNIRGRIN	Simple Ratio Nir/Green	https://www.indexdatabase.de/db/s-single.php?id=168
62	SRNIRRED	Simple Ratio Nir/Red	https://www.indexdatabase.de/db/s-single.php?id=168
63	SRNIRSWIR2	Simple Ratio Nir/Mir	https://www.indexdatabase.de/db/s-single.php?id=168
64	SRREDGREEN	Simple Ratio Red/Green	https://www.indexdatabase.de/db/s-single.php?id=168
65	SRREDNIR	Simple Ratio Red/Nir	https://www.indexdatabase.de/db/s-single.php?id=168
66	SRSWIR	Simple Ratio Mir/Nir	https://www.indexdatabase.de/db/s-single.php?id=168
67	SRSWIRRED	Simple Ratio Mir/Red	https://www.indexdatabase.de/db/s-single.php?id=168
68	TCV	Tasselled Cap - Vegetation	https://www.indexdatabase.de/db/s-single.php?id=168
69	TCW	Tasselled Cap - Wetness	https://www.indexdatabase.de/db/s-single.php?id=168
70	TVI	Transformed Vegetation Index	by Fabian Faßnacht, 2011
71	VARIG	Visible Atmospherically Resistant Index Green	https://www.indexdatabase.de/db/s-single.php?id=168
72	WDRVI	Wide Dynamic Range Vegetation Index	https://www.indexdatabase.de/db/s-single.php?id=168

Tab.2: Time-periods chosen for serial time analysis

Period:			Day diff.		
1	09.02.2016	16.02.2016	<17	In-situ available date 03-05.2016	wet season
2	28.03.2016	20.04.2016	<17		dry season
3	29.04.2016	06.05.2016	<17		
4	22.05.2016	16.06.2016	<17		
5	09.07.2016	18.07.2016	<17		
6	03.08.2016	10.08.2016	<17		
7	19.08.2016	26.08.2016	<17		
8	04.09.2016	27.09.2016	<17		
9	22.10.2016	29.10.2016	<17		

Tab.3: Ordered Landsat 8 Level 2 data

row	date	path_169 (76-77)	path_168 (76-78)	cloud cover
76	20160209		LC08_L1TP_168076_20160209_20170405_01_T1	<20%
77	20160209		LC08_L1TP_168077_20160209_20170405_01_T1	<10%
78	20160209		LC08_L1TP_168078_20160209_20170405_01_T1	<10%
76	20160216	LC08_L1TP_169076_20160216_20170329_01_T1		<10%
77	20160216	LC08_L1TP_169077_20160216_20170329_01_T1		<10%
78				
76	20160328		LC08_L1TP_168076_20160328_20170327_01_T1	<10%
77	20160328		LC08_L1TP_168077_20160328_20170327_01_T1	<10%
78	20160328		LC08_L1TP_168078_20160328_20170327_01_T1	<10%
76	20160420	LC08_L1TP_169076_20160420_20170326_01_T1		<10%
77	20160420	LC08_L1TP_169077_20160420_20170326_01_T1		<10%
78				
76	20160429		LC08_L1TP_168076_20160429_20170326_01_T1	<10%
77	20160429		LC08_L1TP_168077_20160429_20170326_01_T1	<10%
78	20160429		LC08_L1TP_168078_20160429_20170326_01_T1	<10%
76	20160506	LC08_L1TP_169076_20160506_20170325_01_T1		<10%
77	20160506	LC08_L1TP_169077_20160506_20170325_01_T1		<10%
78				
76	20160522	LC08_L1TP_169076_20160522_20170324_01_T1		<10%
77	20160522	LC08_L1TP_169077_20160522_20170324_01_T1		<10%
78	20160522			
76	20160616		LC08_L1TP_168076_20160616_20170323_01_T1	<10%
77	20160616		LC08_L1TP_168077_20160616_20170323_01_T1	<10%
78	20160616		LC08_L1TP_168078_20160616_20170323_01_T1	<10%
76				
77	20160709	LC08_L1TP_169076_20160709_20170323_01_T1		<10%
78	20160709	LC08_L1TP_169077_20160709_20170323_01_T1		<10%
76	20160718		LC08_L1TP_168076_20160718_20170323_01_T1	<10%
77	20160718		LC08_L1TP_168077_20160718_20170323_01_T1	<10%
78	20160718		LC08_L1TP_168078_20160718_20170323_01_T1	<10%
76	20160803		LC08_L1TP_168076_20160803_20170322_01_T1	<10%
77	20160803		LC08_L1TP_168077_20160803_20170322_01_T1	<10%
78	20160803		LC08_L1TP_168078_20160803_20170322_01_T1	<10%
76	20160810	LC08_L1TP_169076_20160810_20170322_01_T1		<10%
77	20160810	LC08_L1TP_169077_20160810_20170322_01_T1		<10%
78				

Tab.3-2

76	20160819		LC08_L1TP_168076_20160819_20170322_01_T1	<10%
77	20160819		LC08_L1TP_168077_20160819_20170322_01_T1	<10%
78	20160819		LC08_L1TP_168078_20160819_20170322_01_T1	<10%
76	20160826	LC08_L1TP_169076_20160826_20170322_01_T1		<10%
77	20160826	LC08_L1TP_169077_20160826_20170322_01_T1		<10%
78				
76	20160904		LC08_L1TP_168076_20160904_20170321_01_T1	<10%
77	20160904		LC08_L1TP_168077_20160904_20170321_01_T1	<10%
78	20160904		LC08_L1TP_168078_20160904_20170321_01_T1	<10%
76	20160927	LC08_L1TP_169076_20160927_20170320_01_T1		<10%
77	20160927	LC08_L1TP_169077_20160927_20170320_01_T1		<10%
78				
76	20161022		LC08_L1TP_168076_20161022_20170319_01_T1	<10%
77	20161022		LC08_L1TP_168077_20161022_20170319_01_T1	<10%
78	20161022		LC08_L1TP_168078_20161022_20170319_01_T1	<20%
76	20161029	LC08_L1TP_169076_20161029_20170319_01_T1		<10%
77	20161029	LC08_L1TP_169077_20161029_20170319_01_T1		<10%
78				